

# Design and Energetic Characterization of a Solenoid Injected Liquid Monopropellant Powered Actuator for Self-Powered Robots

Bobby Shields and Michael Goldfarb  
*Department of Mechanical Engineering  
Vanderbilt University  
Nashville, TN 37235 USA  
email: goldfarb@yuse.vanderbilt.edu*

**Abstract** - This paper describes a direct-injection, liquid monopropellant powered actuation system, which was developed for the purpose of providing mechanical power to self-powered human-scale robots. The actuation system utilizes the catalytic decomposition of a monopropellant as a hot gas generator for powering pneumatic-type actuators. Specifically, pressurization of a pneumatic actuator is provided via solenoid injection valves, which control the flow of the monopropellant through a catalyst pack into the respective sides of the cylinder. Depressurization is provided by a three-way proportional spool valve, which can exhaust one of the two cylinder chambers. A prototype of the actuation system is described, and experimental data is presented that demonstrates good force and motion tracking performance. Experimental results characterizing the energetic performance of the system demonstrate that the prototype provides an energetic figure of merit an order of magnitude greater than that of battery-powered servomotors.

**Index Terms** - Actuators, human-scale robot, hydrogen peroxide, monopropellant, self-powered robot

## I. INTRODUCTION

### A. Motivation

One of the main challenges concerning the development of self-powered, human-scale robots is the need for a power supply that provides adequate energy and power densities in order for the robot to perform significant work for an extended period of time. One of the most common actuation systems used for robots are servomotors powered by batteries. Battery powered servomotors provide good controllability and convenient packaging. Based upon current battery technology, however, the weight of batteries and motors needed to perform useful work for an extended period of time is excessive. A state-of-the-art example of a human-scale robot that utilizes batteries and servomotors is the Honda Motor Corporation humanoid robot model P3. This robot has a total mass of 130 kg (285 lb), of which 30 kg (66 lb) are nickel-zinc batteries. This amount of batteries provides enough power for approximately 15-25 minutes of operation, depending upon the workload. Such durations of operation limit considerably the utility of these robots. The motivation for this work is to develop an actuation system for a self-powered, human-scale robot that allows it to operate for much longer durations than current battery-powered servomotors allow.

The primary motivation for the work presented herein is to develop a power supply and actuation system with a control bandwidth appropriate for use in human scale robots, but with considerably (i.e., order of magnitude) better energetic properties. In order to quantitatively compare the energetic capability of power supply and actuation systems, one must determine an appropriate figure of merit. Gabrielli and von Karman proposed an energetic figure of merit appropriate for mobile robots, called specific resistance, which essentially characterizes the locomotive efficiency as the average power required for locomotion, divided by the locomotion speed and weight of the robot, vehicle, or organism [1]. This figure of merit, however, is a high-level measure that includes locomotive strategy among other factors, and fails to explicitly isolate the energetic performance of the power supply and actuation system from the rest of the low and high level factors affecting locomotive efficiency. Generalized measures of the energetic performance of power supply and actuation systems are nearly absent from the literature. A recent publication by Goldfarb et al. [2] proposes an energetic figure of merit called the actuation potential, which is adopted in this paper as well. The actuation potential consists simply of the product of three measures: the energy density of the power source, the efficiency of energy conversion from the power source to controlled mechanical energy in the joint space, and the power density of the actuator. The actuation potential is given by:

$$A_p = e_s \eta p_a \quad (1)$$

where  $e_s$  is the mass-specific energy density of the power source,  $\eta$  is the efficiency of energy conversion from the power source to controlled mechanical work, and  $p_a$  is the maximum mass specific power density of the actuation system. As pointed out in [2], this performance index represents a figure of merit that is justified by the fact that a system with high power-source energy density, high conversion efficiency, and high actuator power density will be the lightest possible system capable of delivering a given amount of power and energy. For a battery-powered servomotor actuation system, the energy density  $e_s$  of the power source is the electrical energy density of the battery, the efficiency  $\eta$  is the combined efficiency of the servomotor and the gearhead, and the mass specific power density of the

actuation system  $p_a$  is the maximum (continuous) output power of the motor/gearhead divided by its mass.

### B. Monopropellant Powered Approach

Thermochemical reactions, such as combustion, can provide significantly greater energy density than electrochemical ones. A typical thermochemical reaction incorporates a fuel and an oxidizer, along with some activation energy, to produce some reaction product and heat. One problem with such reactions, however, is that the heat must be converted into controlled mechanical work in order to power a robot. Since heat can be efficiently transduced into pressure via the constitutive nature of gaseous reaction products, and since fluid-powered systems (i.e., hydraulic and pneumatic actuators) transduce pressure into mechanical work, a thermochemical/fluid-powered actuator combination offers the potential of a high energy density source and a high power density actuator.

Many classes of thermochemical reactions exist, including hydrocarbon fuel and air mixtures, non-air-breathing bipropellants (e.g., liquid oxygen and liquid hydrogen rocket engines), various solid propellants, and liquid or gas monopropellants. The latter three include all reactants in a single component, and are distinguished from one another principally by their phase. Some liquid and gas monopropellants offer the possibility of reaction without explicitly adding activation energy. Rather, for this class of propellant, the reaction can be initiated solely by the presence of a catalyst. The actuation system described in this paper utilizes one such monopropellant, hydrogen peroxide, which decomposes exothermically in the presence of various catalysts. One attractive feature of such reactions for the purpose of a robotic actuation system is that the rate of energy release, or power, can be controlled simply by controlling the flow rate of the liquid propellant through the catalyst. As such, assuming a sufficiently fast reaction, the power supplied by the reaction can be controlled at a bandwidth appropriate for robotic actuation. Modulating the power production directly eliminates the need for dissipative control action, which typically accounts for a significant proportion of the energy required for actuated robots.

Monopropellants have been utilized in several applications involving power and propulsion, mainly to power gas turbine and rocket engines, torpedo propulsion, reaction control thrusters for space vehicles, and auxiliary power turbo pumps for aerospace vehicles [3, 4]. Despite the use of monopropellants in these various applications, the only prior literature found concerning the development of position or force controllable monopropellant-powered actuators is the work done by Goldfarb et al. [2], which utilized the monopropellant hydrogen peroxide as a power source for the position and force control of a pneumatic actuator. The configuration described in [2] is much like a standard pneumatic actuation system, but utilizes the monopropellant gas generator in place of an air compressor. Specifically, that configuration incorporated a solenoid valve to meter the flow of hydrogen peroxide through a catalyst pack and into a high-pressure hot gas reservoir. Like a conventional pneumatic actuation system, a four-way proportional spool valve controls the flow of compressible fluid (in this case a hot gas) from the reservoir into one side

of a pneumatic piston while exhausting the other side to atmosphere. As such, the monopropellant reaction was used to provide low bandwidth power, while control of a spool valve was used to provide high bandwidth mechanical output power. Such a system provides effective control and was experimentally shown to provide an actuation potential five times greater than a battery/servomotor combination with a low concentration propellant [2]. Despite such promise, the system presented in [2] does not take full advantage of the monopropellant power source. Specifically, as previously mentioned, incorporating a dissipative control element such as a spool valve will, in general, significantly decrease the efficiency of energy conversion. Rather than control energy release at a low bandwidth and modulate the output power with a dissipative valve, one can alternatively control energy release from the monopropellant at a high bandwidth, and thus eliminate the dissipative modulation element, resulting in a greater conversion efficiency and high actuation potential. The work presented in this paper incorporates such a configuration, called a direct injection configuration, a schematic of which is shown in Fig. 1. In this configuration, pressurized propellant is injected via solenoid injection valves through catalyst packs directly into the respective sides of a pneumatic cylinder. The cylinder chambers are depressurized via a proportional three-way spool valve, which can exhaust one cylinder chamber or the other at any given time. Note that proportional injection valves with the required flow rate, speed, and size specifications are not commercially available. Note that in this configuration, the power loss due to fluid throttling at the injection valves is insignificant (i.e., the fuel flow rates are orders of magnitude lower than the gas flow rates), and as such, control losses are essentially eliminated (note that exhaust valve control losses are neglected, since any remaining energy in the exhaust products would be discarded in any case).

A prototype of the direct injection actuator depicted in Fig. 1 was fabricated and used to actuate the single degree of freedom arm shown in Fig. 2. The prototype was built to demonstrate the position and force tracking control of the actuator and to conduct experiments that characterize the actuation potential as given by (1). As shown in the figures, the monopropellant hydrogen peroxide is stored in a stainless steel blow down tank pressurized to 2068 kPa (300 psig). The fuel is supplied to two injection valve/catalyst pack combinations (one connected to each side of the piston)

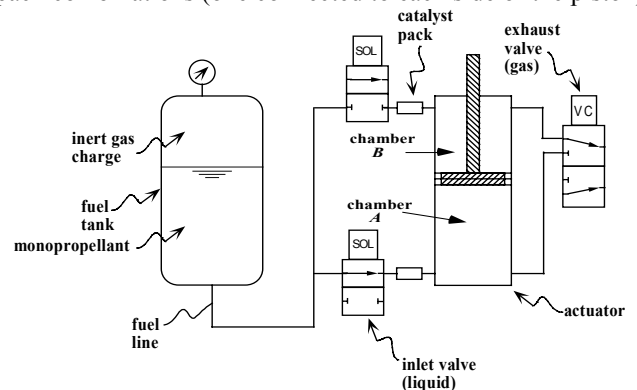


Fig. 1. Schematic of the direct-injection monopropellant based actuation system.

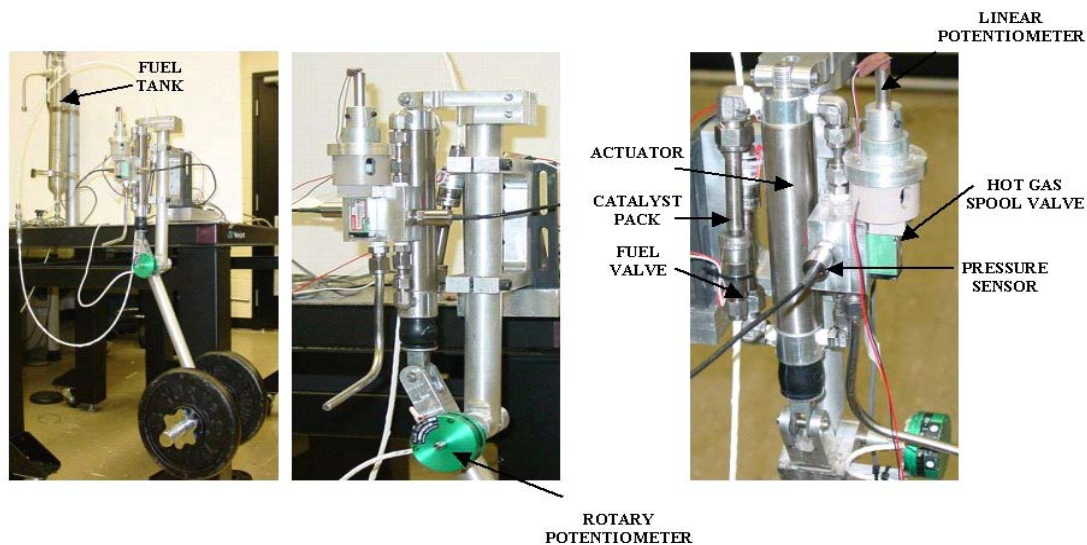


Fig. 2. Single degree-of-freedom manipulator with monopropellant-based actuation prototype.

via flexible fuel lines. The solenoid-actuated on/off injection valves (Parker/General Valve model 009-581-050-2) are capable of one-millisecond minimum opening durations. Each catalyst pack consists of a 5 cm (2 in) long, 1 cm (3/8 in) diameter stainless steel tube packed with iridium-coated alumina granules. The gaseous reaction products from the catalyst packs are injected into either side of a 2.7 cm (1.0625 in) diameter, 10 cm (3.9 in) stroke, double-acting single rod pneumatic actuator (Bimba model 094-DX). A pair of pressure sensors (Entran model #EPXT) are used to measure the chamber pressures (one for each side). A three-way spool valve provides for depressurization of the cylinder chambers, though only one chamber can be depressurized at any given time. The proportional hot gas spool valve was constructed by using the spool, sleeve, and body of a commercially available solenoid-actuated valve (Numatics Microair model #M11SA441M), and replacing its standard solenoid actuator with a thermally isolated voice coil (BEI model #LA10-12-027A) and incorporating a linear potentiometer (Midori model #LP10-FQ), which provides closed-loop control of the exhaust valve spool position with a bandwidth in excess of 10 Hz. The actuator is kinematically arranged to produce a bicep-curling motion upon extension of the piston rod, where the arm angle is measured with a rotary potentiometer (Midori model #CPP-45) to enable for closed-loop servo control. Finally, note that this experimental prototype utilizes a 70% concentration of hydrogen peroxide (70% peroxide, 30% water, by weight). Since the actuation potential scales with the lower heating value of the propellant, one would prefer to use the highest concentration possible. As the concentration increases, however, the adiabatic reaction temperature also increases (in a nonlinear fashion). As such, the concentration of the propellant is limited by the maximum operating temperatures of the respective commercial components used on the prototype. The adiabatic reaction temperature of 70% peroxide is 232°C (453°F), which is at the operating limit of several of the materials in the prototype. Incorporating significantly higher propellant concentrations would thus require the development of

hardware components capable of withstanding higher temperatures. As such, all experiments presented in this paper were performed using 70% hydrogen peroxide.

## II. ACTUATOR CONTROL

A force controller was developed to provide a low level actuator force control, around which an appropriate motion controller can be designed. The force controller consists of three major components: a predictive portion that enables proportional chamber pressurization via the discrete injection valves, a simple pressure feedback controller for chamber depressurization via the proportional exhaust valve, and a supervisory controller that determines the respective pressurization and depressurization rates of each chamber, and coordinates the injection and exhaust processes.

### A. Pressurization Control

Each chamber of the cylinder is pressurized via a binary solenoid valve, capable of either being fully open or fully closed. As such, the (proportional) control of the injection dynamics (i.e., chamber pressurization) must accommodate the discrete nature of the injection valves. Proportional control from a binary input can be achieved in various manners, including pulse-width-modulated control, switching control, and predictive control. Due to the low bandwidth of the valves relative to the reaction/pressurization dynamics, and due to the time delay inherent in these dynamics, a predictive controller was developed as a means to pressurize the cylinder chambers. A predictive controller directly computes the expected output of the system for each possible discrete input at each instant in time, and as such is the most direct method of model-based switching control. The predictive controller used for the injection control predicts the states of the system at an appropriate future time horizon for each of the present-time discrete-valued input candidates (valve off or fully open). The error between the predicted states and the future desired states is calculated for each of the inputs and the input candidate that drives the system closest to the desired states is chosen. This predictive controller is

described in detail in the previous publications [5, 6], and is shown in these publications to provide effective tracking of a desired pressurization trajectory.

### B. Depressurization Control

Depressurization of each respective side of the cylinder is achieved via the control of a three-way proportional spool valve in a manner similar to that of a standard pneumatic servo actuator, and is thus considerably simpler than control of pressurization. In fact, a simple proportional feedback controller that operates on pressure error commands the exhaust valve spool position. This was experimentally shown to provide effective tracking control of cylinder depressurization as shown in [5].

### C. Supervisory Control

The direct injection actuator incorporates three valve commands in order to control a single output (force). As such, a supervisory controller is required to determine the appropriate pressure trajectories and to properly coordinate the respective valves in order to track these trajectories. A block diagram of this supervisory controller is shown in Fig. 3. As shown in the diagram, the controller attempts to obtain a given desired force by pressurizing one chamber at the same rate that the opposite chamber is depressurized. The pressurization rates are integrated to obtain the desired chamber pressures,  $P_{d(A)}$  and  $P_{d(B)}$ , which provide the desired pressures for the respective pressurization and depressurization controllers. The desired pressures are then saturated, since the actual chamber pressures can only vary between atmospheric pressure and the supply pressure of the blow down tank. In addition to providing the desired pressure trajectories, the supervisory controller coordinates the injection and exhaust of the respective chambers. The coordination of valves is achieved by constraining the injection valves to operate asymmetrically (i.e., only one injection valve can be open at any given time), and by disallowing simultaneous charging and exhausting the same chamber. As shown in Fig. 3, these conditions are enforced based on the force error, which is used to determine which of the three valves are active. Specifically, if the force error is positive, injection valve *A* is used to pressurize chamber *A*, and the exhaust valve is used to depressurize chamber *B*. If the force error is negative, injection valve *B* is used to pressurize chamber *B*, and the exhaust valve is used to depressurize chamber *A* (refer to Fig. 1).

### D. Experimental Force and Position Tracking Results

The proposed force controller was implemented within a servo control loop on the prototype actuator shown in Fig 2. Specifically, the actuator was utilized as a force source within a simple proportional-integral-derivative (PID) servo control loop with feedforward gravity compensation. Verifying the performance of the force controller within a servo loop ensured a large variation in the output load and speed. Fig. 4 shows results of the servo control tracking of a 30-degree amplitude, 1 Hz sinusoidal trajectory, with an 11.2 kg (25 lb) load, and Fig. 5 shows the corresponding force control. The tracking of both motion and force indicates the effectiveness of the proposed control approach.

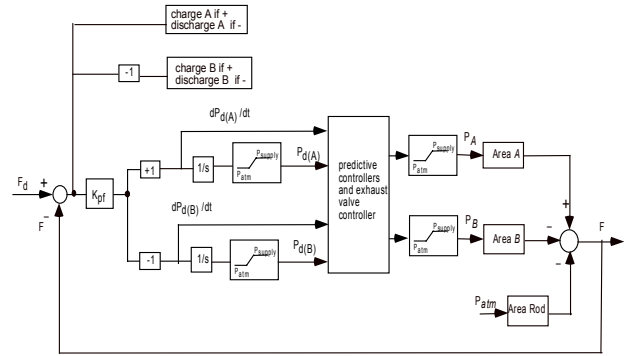


Fig. 3. Supervisory control loop block diagram.

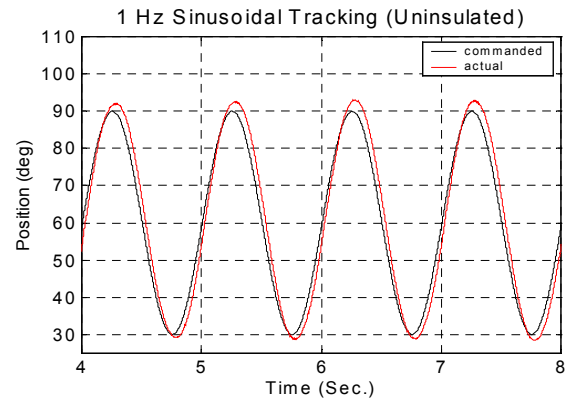


Fig. 4. Closed-loop position tracking of a 1 Hz sinusoid signal, 30-degree amplitude.

Commanded Force for 1 Hz Sinusoidal Tracking vs. Actual Force

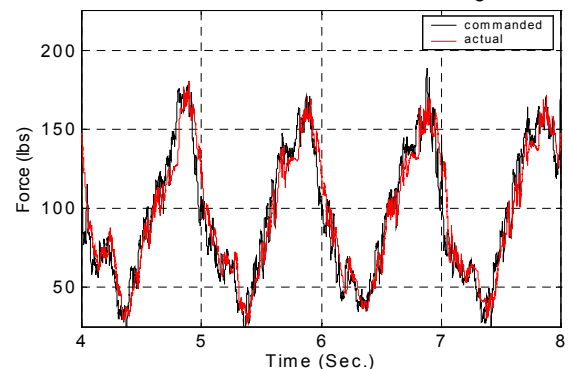


Fig. 5. Force tracking corresponding to the motion control shown in Fig. 4.

## III. ENERGETIC ANALYSIS

As previously mentioned, the primary motivation for this work is to develop an actuation system for a self-powered, human-scale robot that allows it to operate for much longer durations than current battery-powered servomotors. Such a system must provide a significant improvement in actuation potential relative to state-of-the-art batteries and servomotors. As such, experiments were performed to characterize the actuation potential of the proposed system. Regarding the actuation potential, since the mass-specific energy density (i.e., the higher heating value) of the 70% hydrogen peroxide used in the experiments is known, and since the mass of the actuation system is also known, knowledge of the effective energy density of the system requires measurement of the conversion efficiency from the propellant to controlled

mechanical work output. In general, the efficiency of conversion will depend on the characteristics of motion and the nature of the load. In order to approximate a typical motion and load experienced by a humanoid robot, the efficiency of energy conversion was characterized with an inertial load of 11.2 kg (25 lb) at the endpoint, and commanded to track the 1 Hz sinusoidal trajectory shown in Fig. 4. Control of this motion is considered a non-conservative task. Such an assumption is debatable, but since a figure of merit is for purposes of comparison, consistent application of this assumption provides meaningful results. As such, the efficiency of conversion is measured by measuring the average rectified mechanical power output over an even number of cycles, measuring the fuel flow rate over the same period, and using knowledge of the higher heating value to compute the efficiency. Before describing the resulting experimental measurements, it is informative to compute the best possible efficiency under idealized assumptions.

#### A. Thermodynamic Model

The upper bound for the conversion efficiency for the load and trajectory considered here could be calculated using the thermodynamic model developed in [2]. Based on this model, the maximum theoretical conversion efficiency for the motion and load previously described (based on the use of a 70% concentration propellant) is 80%, which is relative to the lower heating value of the propellant. Note that this was presented as 16% in [2], which is relative to the higher heating value. Though the efficiency used in the expression for actuation potential is defined relative to the higher heating value, the efficiency of conversion at the actuator level is more accurately represented by an efficiency expressed relative to the lower heating value. The higher heating value includes energy that must be used to vaporize the water present in the reaction products, and thus includes energy that is not retrievable by an actuator. The lower heating value represents only the retrievable energy in the reaction product, and thus an actuator could theoretically achieve 100% efficiency, relative to the lower heating value. As such, the efficiency of the actuator is characterized relative to the lower heating value, even though the actuation potential requires an efficiency defined relative to the higher heating value. The model utilized to obtain this conversion efficiency assumes no heat loss and no energy loss due to closed-loop control.

#### B. Experiments

Experiments were conducted to measure the actual efficiency in converting the energy stored in the 70% concentration hydrogen peroxide to mechanical work. The controlled mechanical power output was measured via the combination of pressure sensors (used to compute actuator force) and the joint angle potentiometer (used to compute actuator velocity). The instantaneous power was then calculated by

$$\mathbf{P}(t) = |\tau \dot{\theta}| \quad (2)$$

where  $\tau$  is the delivered torque,  $\dot{\theta}$  is the angular velocity of the arm, and the absolute-value operator reflects the fact that the system is assumed energetically nonconservative. The

average power was calculated by integrating over an integer number of cycles  $n$

$$\mathbf{P}_{avg} = \frac{\int_{t_1}^{t_2} \mathbf{P}(t) dt}{t_2 - t_1} \quad (3)$$

where  $\omega(t_2 - t_1) = 2\pi n$ . The mass of monopropellant consumed during the time from  $t_1$  to  $t_2$  was indirectly measured by recording the pressure of the nitrogen gas in the blowdown tank, assuming an isothermal process inside the constant-volume tank, and calculating the volume occupied by the nitrogen from the ideal gas equation, which in turn yields the volume of propellant in the tank. Since the volume and density of the liquid propellant are known, the mass of propellant is easily calculated. The conversion efficiency based upon the lower heating value was calculated by

$$\eta_l = \frac{\mathbf{P}_{avg}(t_2 - t_1)}{e_l m_{H_2O_2}} \quad (4)$$

where  $e_l$  is the lower heating value of 70% hydrogen peroxide and is 0.4 MJ/kg, and  $m_{H_2O_2}$  is the mass of fuel consumed during the time duration from  $t_1$  to  $t_2$ .

For the 1-Hz sinusoidal motion shown in Fig. 4, the trajectory is defined by a starting angle of  $\theta_1 = 30^\circ$  and a final angle of  $\theta_2 = 90^\circ$  (defined relative to the downward vertical). This trajectory was repeated several times in 30-second segments, and the efficiency for each run was found from (4) for the time span from  $t_1 = 4$  sec to  $t_2 = 26$  sec. The first four seconds and the final four seconds of each test were not included because they represent starting and ending transition periods (i.e., the trajectory was ramped up and ramped down). Note that the pressure and volume in chambers *A* and *B* were measured at both the start and end of the efficiency measurement window ( $t_1 = 4$  sec and  $t_2 = 26$  sec), and the pneumatic energy stored in each chamber at these respective instants was calculated (i.e., the product of chamber pressure and volume). The difference in energy stored in the cylinder at  $t_2$  and  $t_1$  was calculated (i.e., the contribution of any stored actuator energy to the output work), and only cases for which this was near zero were considered (i.e., measurements were considered valid if the stored energy constituted less than 0.1% of the total output energy). Based upon these experiments, the efficiency of conversion was found to be  $\eta_l = 51\%$ . This compares favorably to the measured efficiency of  $\eta_l = 33\%$  for the prototype configuration described in [2] (the efficiency given in [2] is relative to the higher heating value and is  $\eta = 6.6\%$ ). With regard to the estimated upper bound, the presence of heat loss, frictional losses, losses due to leakage, some control losses, and imperfect control (i.e., imperfect tracking) in the prototype all contribute to the disparity. Regarding the latter, the model used to obtain the ideal efficiency assumes that no gas is exhausted during a given monotonic segment of the trajectory. However, due to controller inefficiencies, the measured pressure in the piston can overshoot the requisite pressure, causing intermittent exhaust of hot gas from the piston, thus decreasing the conversion efficiency. The existence of this intermittent exhaust is evident in the oscillations exhibited in the power

delivered to the load, and this is shown in Fig. 6 versus the theoretically required power.

### C. Experimentally Determined Actuation Potential

Having measured the conversion efficiency, the mass-specific power density  $p_a$  of the actuator and the mass-specific energy density of the power source (considering the storage tank) need to be determined in order to calculate the actuation potential given by (1). The mass-specific power density was found by measuring the actuator's maximum (measured) deliverable power and dividing this by the measured mass of the actuator. The maximum deliverable power was found experimentally by measuring the instantaneous output power (force and velocity, as previously described) for a step response. The PID gains of the servo control loop were adjusted so that the arm would have the fastest rise-time possible (thus maximizing the power). Since one of the factors that affects the maximum deliverable power is the nature of the load, the experiment was conducted for different end-point masses. The maximum measured deliverable power is 335 W, which was measured with a 7 kg mass attached to the end of the arm. The total mass of the actuation system is 1.2 kg, so the resulting mass-specific power density of the actuator is  $p_a = 279$  W/kg.

Having determined the conversion efficiency and the power density, only the power-source energy density needs to be found in order to calculate the actuation potential. The higher heating value of 70% hydrogen peroxide is approximately 2 MJ/kg [7]. However, the propellant must be stored in a blowdown tank, so the effective energy density of the propellant/tank combination is somewhat lower, as given by

$$e_s = \frac{m_{fuel}e_h}{m_{fuel} + m_{tank}} \quad (5)$$

where  $m_{fuel}$  is the mass of fuel in the tank,  $m_{tank}$  is the mass of the tank, and  $e_h$  is the higher heating value of the fuel. The density of 70% hydrogen peroxide is 1.3 kg/L, so a 10-liter composite tank with a mass of 2 kg will reduce the effective mass-specific energy density of the fuel from 2 MJ/kg to 1.73 MJ/kg. Based upon this value, as well as the measured conversion efficiency of  $\eta = 10.1\%$  (which corresponds to the previously stated  $\eta_t = 51\%$ ), and mass-specific power density  $p_a = 279$  W/kg, the actuation potential for this single-degree-of-freedom system, as given by (1), is  $A_p = 49.2$  kJ·kW/kg<sup>2</sup>. For purposes of comparison, the actuation potential of a servomotor actuator powered by state-of-the-art batteries was found in [2] to be  $A_p = 4.8$  kJ·kW/kg<sup>2</sup>. Therefore, the single-degree-of-freedom experimental setup described herein, with 70% peroxide, exhibited an actuation potential an order of magnitude higher than a state-of-the-art battery/servomotor system.

Note that the actuation potential of the monopropellant-powered actuator could be increased if the 70% concentration hydrogen peroxide were replaced with a higher concentration. In particular, the lower heating value of the propellant increases by 0.4 MJ/kg for each additional 10% in peroxide concentration. As such, the same actuator fueled with 80% peroxide would have an actuation potential approximately twice the actuation potential measured with

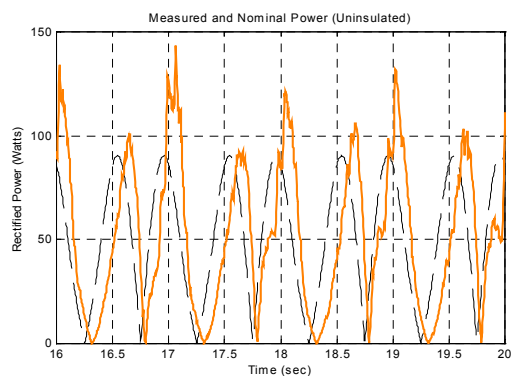


Figure 6. Comparison of the measured power delivered by the actuator (solid) to the theoretically predicted power (dashed) required to track the commanded arm trajectory.

70%. The adiabatic decomposition temperature of 80% peroxide, however, is approximately 487° C (908° F), which is considerably greater than the temperatures incurred by 70% peroxide, and beyond the temperature limits of several of the components in the present prototype. As such, if a greater actuation potential is desired, appropriate fluid power control components must be developed to withstand the corresponding high temperatures.

## IV. CONCLUSIONS

A power supply and actuation system appropriate for the position or force control of a self-powered, human-scale robot was presented. Experimental results indicate that the monopropellant system provides an energetic figure of merit an order of magnitude better than a state-of-the-art battery/servomotor combination. Further, by increasing the propellant concentration, the energetic figure of merit could be increased by almost a factor of four. The use of such propellant, however, would dramatically increase the gas temperatures, and would require the development of custom fluid power components that could withstand the increased temperatures.

## REFERENCES

- [1] Gabrielli, G., von Karman, T. H., "What price speed?" *Mechanical Engineering*, vol. 72, no. 10, pp. 775–781, 1950.
- [2] Goldfarb, M., Barth, E.J., Gogola, M.A., and Wehrmeyer, J.A., "Design and Energetic Characterization of a Liquid-Propellant-Powered Actuator for Self-Powered Robots", *IEEE/ASME Transactions on Mechatronics*, vol. 8, no. 2, pp.254-262, June 2003.
- [3] Wernimont, E.J., Ventura, M., Garboden, G. and Muellens, P., "Past and Present Uses of Rocket Grade Hydrogen Peroxide", *2nd Proceedings of the International Hydrogen Peroxide Propulsion Conference*, pp. 45-67, November 7-10, 1999.
- [4] Koerner, M., "Recent Developments in Aircraft Emergency Power", *Energy Conversion Engineering Conference and Exhibit*, vol. 1, pp. 12-19, July 2000.
- [5] Shields, B.L., Barth, E.J., and Goldfarb, M., "Predictive Pressure Control of a Monopropellant Powered Actuator", *Proceedings of the 2003 ASME International Mechanical Engineering Congress & Exposition*, Washington, D.C., November 15-21, 2003, Paper IMECE 2003-42743.
- [6] Shields, B.L., Goldfarb, M., and Fite, K., "Force and Position Control of a Solenoid Injected Monopropellant-Powered Actuator", *Proceedings of the 2004 ASME International Mechanical Engineering Congress & Exposition*, Anaheim, CA, November 13-19, 2004, Paper IMECE 2004-59442.
- [7] L.H. Dierdorff et al., *Hydrogen Peroxide Physical Properties Data Book*, 2nd edition, Buffalo, NY:Becco Chemical Division, FMC Corporation, 1954.